Ocean Engineering 35 (2008) 1226–1234

Contents lists available at ScienceDirect

Ocean Engineering

journal homepage: www.elsevier.com/locate/oceaneng

Linear wave reflection by trench with various shapes

Tae-Hwa Jung [a,*], Kyung-Duck Suh [b], Seung Oh Lee [c], Yong-Sik Cho [a]

[a] Department of Civil Engineering, Hanyang University, Seoul 133-791, Korea
[b] Department of Civil and Environmental Engineering & Engineering Research Institute, Seoul National University, Seoul 151-744, Korea
[c] School of Urban & Civil Engineering, Hongik University, Seoul 121-791, Korea

ARTICLE INFO

Article history:
Received 14 May 2007
Accepted 3 April 2008
Available online 6 April 2008

Keywords:
Trench
Analytical solution
Mild-slope equation
Bragg reflection

ABSTRACT

Two types of analytical solutions for waves propagating over an asymmetric trench are derived. One is a long-wave solution and the other is a mild-slope solution, which is applicable to deeper water. The water depth inside the trench varies in proportion to a power of the distance from the center of the trench (which is the deepest water depth point and the origin of x-coordinate in this study). The mild-slope equation is transformed into a second-order ordinary differential equation with variable coefficients based on the longwave assumption [Hunt's, 1979. Direct solution of wave dispersion equation. Journal of Waterway, Port, Coast. and Ocean Engineering 105, 457–459] as approximate solution for wave dispersion. The analytical solutions are then obtained by using the power series technique. The analytical solutions are compared with the numerical solution of the hyperbolic mild-slope equations. After obtaining the analytical solutions under various conditions, the results are analyzed.

1. Introduction

Wave reflection due to a bathymetric change has been rigorously investigated as one of the credible methods to protect coastal areas from severe wave attacks. In general, practical tools such as numerical, experimental or analytical methods are frequently used to predict and analyze wave reflection. Among those methods, we focus our interest on an analytical approach which has the advantage of obtaining solutions quickly, simply and accurately, although they are only available for idealized situations. And it can be used to compare and verify the results from other methods.

Lamb (1932, p. 262, Art. 176) first presented the long-wave solution to the reflection or transmission of waves for a finite step by using matching conditions for surface and normal mass flux at the boundary. Takano (1960) developed the analytical solution for arbitrarily varying water depths, which can be expressed as a series of small steps by using the eigenfunction expansion method. His approach, in fact, originated from Bremmer (1951) who had described the wave solution using WKBJ (or Liouville-Green) approximation in electromagnetic waves. The method suggested by Takano (1960) was also used by Kirby and Dalrymple (1983), Liu et al. (1992) and Cho and Lee (2000). Dean (1964) obtained the long-wave solution by solving the continuity and the Euler equations in which the water depth or channel width was assumed to vary linearly. He found that the governing equation was transformed into the Bessel equation in the linear transition of water depth or channel width and thus the solution was expressed as a Bessel function. Dean's (1964) solutions become identical with those of Lamb (1932) when the slope changes abruptly. Miles (1967) introduced the scattering matrix to calculate the reflection and transmission coefficients using the variational principle and applied his method to a continental shelf. Later, Devillard et al. (1988) developed the theoretical solution for the wave reflection and transmission over arbitrarily varying topography using the transfer matrix, which renormalized the scattering matrix. His approach was similar to Bremmer (1951) or Takano (1960). He divided the domain into small steps having constant water depth and applied the transfer matrix to each step.

Lee and Ayer (1981) investigated the symmetric trench problem using the transform method. And for similar geometry, Miles (1982) calculated the diffraction of a long surface wave by a deformation of the bottom through a conformal-mapping algorithm proposed by Kreisel (1949). He applied his results to the symmetric rectangular trench. In order to consider obliquely incident waves, Miles (1982) used the variational method developed by Mei and Black (1969).

For the case of an asymmetric rectangular trench, Lassiter (1972) and Kirby and Dalrymple (1983) derived an analytical solution by using the variational method and Takano's (1960) method, respectively. Bender and Dean (2003) studied the

* Corresponding author. Tel.: +82 2 2220 0559.
E-mail address: togye176@paran.com (T.-H. Jung).

0029-8018/$ - see front matter © 2008 Elsevier Ltd. All rights reserved.
doi:10.1016/j.oceaneng.2008.04.001

reflection and transmission of normally incident waves by the trench and shoals with sloped transitions. They developed two methods, the step method and the slope method, using the linearized theory. The step method is an extension of the solution of Takano (1960) and it can be applied to arbitrary water depths assuming the sloped transition as a series of steps. The slope method is an extension of Dean's (1964) method that allows a trench and shoals with a linear transition between changes in depth but valid only within the long-wave region. Recently, Lin and Liu (2005) and Chang and Liou (2007) conducted analytical studies for the long-wave reflection by trapezoidal shape breakwaters by modifying Dean's (1964) solution.

In this study, the analytical solutions propagating over the trench having various shapes including linear and abrupt change of depth are developed by using the power series. One is a long-wave solution, which is valid only for shallow water, and the other is a mild-slope solution, which is valid for both shallow and deep-water depths. The series solution approach considered in this study is frequently used in two-dimensional horizontal analytical problems since Zhang and Zhu (1994) first proposed that approach for the propagation of long waves around a conical island and over a parabolic shoal. We apply the series solution to a two-dimensional vertical problem to consider the wave reflection and transmission by a trench. To develop the mild-slope solution, Hunt's (1979) approximate solution for the wave dispersion given by Liu et al. (2004) is employed. Hunt's approximate solution was also used to develop an analytical solution for the submerged truncated paraboloidal shoal by Lin and Liu (2007). In the following section, the analytical solutions to the mild-slope equation are derived and then compared with the numerical solution based on the same governing equation. Finally, the results obtained from analytical solutions applied to various shapes of trench are investigated.

2. Analytical solutions

The flow domain of interest is divided into the constant flow depth regions (I, IV) and the variable flow depth regions (II, III) to consider the wave deformation in two-dimensional vertical problems. For simplicity and convenience, the positive direction in the horizontal and vertical coordinates is defined as the right side from the trench center and upward from the still-water level, respectively as shown, in Fig. 1. h_0 is the water depth at the center of a trench, h_1 and h_2 are the constant depths, a_1 and a_2 are the distances from the center of a trench to the imaginary edge of a trench extended to the water surface, respectively, b_1 and b_2 are the distances from the center of a trench to the actual edges of a trench, and α is an arbitrary positive integer. Fig. 1 is an example for the case of $\alpha = 1, 2$, and ∞. As shown in Fig. 1, the side slope of a trench is linear for $\alpha = 1$, and parabolic for $\alpha = 2$, and it becomes a vertical step for $\alpha = \infty$.

Considering a homogeneous incompressible and inviscid fluid with irrotational motion traveling over an asymmetric trench, the (time-harmonic) mild-slope equation can become the governing equation of interest.

$$\frac{\mathrm{d}}{\mathrm{d}x}\left(CC_g\frac{\mathrm{d}\eta}{\mathrm{d}x}\right)+\sigma^2\frac{C_g}{C}\eta=0 \tag{1}$$

where η is the complex amplitude of the water surface elevation, C the phase velocity, C_g the group velocity, and σ the wave angular frequency.

To solve the boundary problem, appropriate boundary conditions should be required. The continuity of surface elevation and its derivative are used to conserve the mass and momentum at the junction where each region meets and the radiation condition is used at $x = \pm\infty$.

In the constant-water-depth regions (I and IV), the form of the solution of Eq. (1) is

$$\eta = A\mathrm{e}^{\mathrm{i}kx} + B\mathrm{e}^{-\mathrm{i}kx} \tag{2}$$

where A and B are unknown complex variables to be determined by boundary conditions, k is the wave number, and i is the pure imaginary number ($\sqrt{-1}$). If waves having unit amplitude are propagating from the left side to the right side in the horizontal coordinate, the water surface elevations in regions I and IV can be expressed, respectively, as.

$$\eta_{\mathrm{I}} = \mathrm{e}^{\mathrm{i}k_1(x+b_1)} + R\mathrm{e}^{-\mathrm{i}k_1(x+b_1)} \quad (x \leqslant -b_1) \tag{3}$$

$$\eta_{\mathrm{IV}} = T\mathrm{e}^{\mathrm{i}k_2(x-b_2)} \quad (x > b_2) \tag{4}$$

where subscripts I and IV are the upwave and downwave constant water depth regions, respectively. R and T represent the reflection and transmission coefficients, and k_1 and k_2 are the wave numbers corresponding to h_1 and h_2, respectively.

In the variable-water-depth regions (II and III), the water depths can be given by

$$h = \begin{cases} h_0\left(1-\dfrac{|x|^{\alpha_1}}{a_1^{\alpha_1}}\right) = h_0\left(1-(-1)^{\alpha_1}\dfrac{x^{\alpha_1}}{a_1^{\alpha_1}}\right), & (-b_1 < x \leqslant 0) \\ h_0\left(1-\dfrac{x^{\alpha_2}}{a_2^{\alpha_2}}\right), & (0 < x \leqslant b_2) \end{cases} \tag{5}$$

where α_1 and α_2 are the values of α on the left and right sides of the trench, respectively.

In this study, two kinds of analytical solution in the variable water depth are developed. One is the long-wave solution, which is valid only in shallow water; the other is the mild-slope solution, which can be applied to from shallow water to deep water.

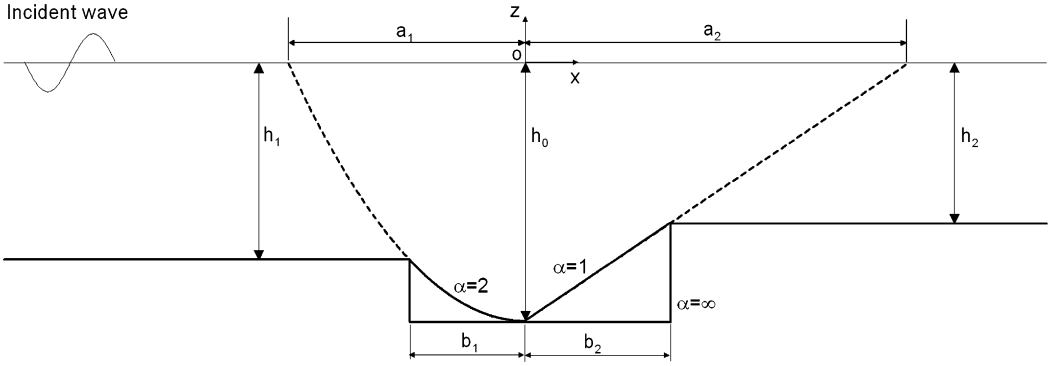

Fig. 1. Definition sketch of an asymmetric trench (for $\alpha = 1, 2$, and ∞).

2.1. Shallow-water model

For long waves, $C \cong C_g = \sqrt{gh}$ and $\sigma^2 = gk^2h$; thus, Eq. (1) in the trench becomes the well-known long-wave equation:

$$h\frac{d^2\eta}{dx^2}+\frac{dh}{dx}\frac{d\eta}{dx}+\frac{\sigma^2}{g}\eta=0 \tag{6}$$

where g is the gravitational acceleration, and h is the water depth inside the trench, which decreases gradually from the center to the edge according to Eq. (5). The trench is assumed to be infinitely long in the y-direction.

Substituting Eq. (5) into Eq. (6) results in the following equations:

$$(a_1^{\alpha_1}-(-1)^{\alpha_1}x^{\alpha_1})\frac{d^2\eta_{II}}{dx^2}-\alpha_1(-1)^{\alpha_1}x^{\alpha_1-1}\frac{d\eta_{II}}{dx}+\nu_1^2\eta_{II}=0 \quad (-b_1<x\leqslant 0) \tag{7}$$

$$(a_2^{\alpha_2}-x^{\alpha_2})\frac{d^2\eta_{III}}{dx^2}-\alpha_2x^{\alpha_2-1}\frac{d\eta_{III}}{dx}+\nu_2^2\eta_{III}=0 \quad (0<x\leqslant b_2) \tag{8}$$

where η_{II} and η_{III} are the water surface elevation inside the trench, and

$$\nu_i=\sqrt{\frac{\sigma^2a_i^{\alpha_i}}{gh_0}} \quad (i=1,2) \tag{9}$$

Since Eqs. (7) and (8) are the second-order ordinary differential equations with variable coefficients, the solutions of Eqs. (7) and (8) can be written in the form of power series as follows:

$$\eta_{II}=\sum_{m=0}^{\infty}\beta_m x^m \quad (-b_1<x\leqslant 0) \tag{10}$$

$$\eta_{III}=\sum_{m=0}^{\infty}\gamma_m x^m \quad (0<x\leqslant b_2) \tag{11}$$

where β_m and γ_m are unknown complex values. These values must be complex because the free surfaces in the variable-depth regions [i.e., Eqs. (10) and (11)] must satisfy the matching conditions at the boundaries with the constant-depth regions (i.e., at $x=-b_1$ and $x=b_2$) and the free surfaces at the constant-depth regions are expressed as complex as shown in Eqs. (3) and (4). These values are determined from recursion relations. According to the Frobenius theory (Hildebrand, 1976), if the series is expanded at ordinary or regular singular points, the series solution converges for $|x-x_0|<X$ where x_0 is ordinary or regular singular point and X is the distance from $x=x_0$ to the nearest singular point ($x_0=0$, $X=a_i$ $(i=1,2)$ in this case). Thus, the solutions of Eqs. (7) and (8) always converge in the whole trench region because the absolute value of b_i is always less than that of a_i as shown in Fig. 1.

Substituting Eqs. (10) and (11) into Eqs. (7) and (8), respectively, and collecting the terms of the same power of x gives the following results:

For $\alpha_i=1$,

$$\beta_m=\frac{-(m-1)^2\beta_{m-1}-\nu_1^2\beta_{m-2}}{a_1m(m-1)} \quad (m\geqslant 2) \tag{12}$$

$$\gamma_m=\frac{(m-1)^2\beta_{m-1}-\nu_2^2\beta_{m-2}}{a_2m(m-1)} \quad (m\geqslant 2) \tag{13}$$

For $\alpha_i=2$,

$$\beta_m=\frac{(m-2)(m-1)-\nu_1^2}{a_1^2m(m-1)}\beta_{m-2} \quad (m\geqslant 2) \tag{14}$$

$$\gamma_m=\frac{(m-2)(m-1)-\nu_2^2}{a_2^2m(m-1)}\gamma_{m-2} \quad (m\geqslant 2) \tag{15}$$

For $\alpha_i\geqslant 3$

$$\beta_m=-\frac{\nu_1^2}{a_1^{\alpha_1}m(m-1)}\beta_{m-2} \quad (2\leqslant m<\alpha_1) \tag{16}$$

$$\beta_m=\frac{(-1)^{\alpha_1}(m-\alpha_1)(m-1)\beta_{m-\alpha_1}-\nu_1^2\beta_{m-2}}{a_1^{\alpha_1}m(m-1)} \quad (m\geqslant\alpha_1) \tag{17}$$

$$\gamma_m=-\frac{\nu_2^2}{a_2^{\alpha_2}m(m-1)}\gamma_{m-2} \quad (2\leqslant m<\alpha_2) \tag{18}$$

$$\gamma_m=\frac{(m-\alpha_2)(m-1)\gamma_{m-\alpha_2}-\nu_2^2\gamma_{m-2}}{a_2^{\alpha_2}m(m-1)} \quad (m\geqslant\alpha_2) \tag{19}$$

where β_0, β_1, γ_0, and γ_1 are arbitrary complex constants. Since the values of β_i and γ_i $(i\geqslant 2)$ are determined by β_0, β_1, γ_0, and γ_1, Eqs. (10) and (11) can be rearranged as follows:

$$\eta_{II}=\beta_0X_1(x)+\beta_1X_2(x) \tag{20}$$

$$\eta_{III}=\gamma_0X_3(x)+\gamma_1X_4(x) \tag{21}$$

where $X_1(x)$ is obtained after choosing $\beta_0=1$ and $\beta_1=0$, and $X_2(x)$ is computed when $\beta_0=0$ and $\beta_1=1$ from Eq. (10). $X_3(x)$ and $X_4(x)$ can be obtained according to the same procedure. The expression for $X_1(x)$ and $X_2(x)$ for the case of $\alpha_1=1$ is given in Appendix A.

Matching conditions at the junction ($x=-b_1$, 0, b_2) give six algebraic equations; thus the unknown coefficients can be obtained using the matrix.

$$\begin{bmatrix}R\\ \beta_0\\ \beta_1\\ \gamma_0\\ \gamma_1\\ T\end{bmatrix}=\begin{bmatrix}a_{11}&a_{12}\\ a_{21}&a_{22}\\ a_{31}&a_{32}\\ a_{41}&a_{42}\\ a_{51}&a_{52}\\ a_{61}&a_{62}\end{bmatrix}\begin{bmatrix}1\\ ik_1\end{bmatrix} \tag{22}$$

where

$$\begin{bmatrix}a_{11}&a_{12}&a_{13}&a_{14}&a_{15}&a_{16}\\ a_{21}&a_{22}&a_{23}&a_{24}&a_{25}&a_{26}\\ a_{31}&a_{32}&a_{33}&a_{34}&a_{35}&a_{36}\\ a_{41}&a_{42}&a_{43}&a_{44}&a_{45}&a_{46}\\ a_{51}&a_{52}&a_{53}&a_{54}&a_{55}&a_{56}\\ a_{61}&a_{62}&a_{63}&a_{64}&a_{65}&a_{66}\end{bmatrix}$$

$$=\begin{bmatrix}-1&X_1(-b_1)&X_2(-b_1)&0&0&0\\ ik_1&X_1'(-b_1)&X_2'(-b_1)&0&0&0\\ 0&X_1(0)&X_2(0)&-X_3(0)&-X_4(0)&0\\ 0&X_1'(0)&X_2'(0)&-X_3'(0)&-X_4'(0)&0\\ 0&0&0&X_3(b_2)&X_4(b_2)&-1\\ 0&0&0&X_3'(b_2)&X_4'(b_2)&-ik_2\end{bmatrix}^{-1} \tag{23}$$

Substituting these coefficients back into Eqs. (3), (4), (20), and (21), the water surface elevation can be obtained for the whole domain. Note that the matching conditions at $x=0$ give $\beta_0=\gamma_0$ and $\beta_1=\gamma_1$. Therefore, the reflection and transmission coefficients

in Eq. (22) can be simplified as follows:

$$R = \frac{-k_1k_2X_2(-b_1)X_3(b_2) - ik_2X_2'(-b_1)X_3(b_2) + k_1k_2X_1(-b_1)X_4(b_2)}{\Delta} + \frac{ik_2X_1'(-b_1)X_4(b_2) - ik_1X_2(-b_1)X_3'(b_2) + X_2'(-b_1)X_3'(b_2)}{\Delta} + \frac{ik_1X_1(-b_1)X_4'(b_2) - X_1'(-b_1)X_4'(b_2)}{\Delta} \quad (24)$$

$$T = \frac{2ik_1[-X_4(b_2)X_3'(b_2) + X_3(b_2)X_4'(b_2)]}{\Delta} \quad (25)$$

where

$$\Delta = -k_1k_2X_2(-b_1)X_3(b_2) + ik_2X_2'(-b_1)X_3(b_2) + k_1k_2X_1(-b_1)X_4(b_2) - ik_2X_1'(-b_1)X_4(b_2) - ik_1X_2(-b_1)X_3'(b_2) - X_2'(-b_1)X_3'(b_2) + ik_1X_1(-b_1)X_4'(b_2) + X_1'(-b_1)X_4'(b_2) \quad (26)$$

2.2. Extension to deeper waters

For the analysis of deeper water, it is advantageous to rewrite the mild-slope Eq. (1) in the following form:

$$CC_g\frac{d^2\eta}{dx^2} + \frac{d(CC_g)}{dx}\frac{d\eta}{dx} + \sigma^2\frac{C_g}{C}\eta = 0 \quad (27)$$

The coefficients in Eq. (27), expressed with the phase velocity and the group velocity, involve the wave number that must be obtained from the implicit linear dispersion relation. This makes it difficult to solve Eq. (27) analytically. To make the coefficients in Eq. (27) be explicit in forms, Hunt's (1979) direct solution is employed in this study. It involves an infinite series while taking the following form:

$$(kh)^2 = \xi^2 + \frac{\xi}{P(\xi)} \quad (28)$$

$$P(\xi) = 1 + \frac{2}{3}\xi + \frac{16}{45}\xi^2 + \frac{152}{945}\xi^3 + \frac{128}{2025}\xi^4 + \cdots \quad (29)$$

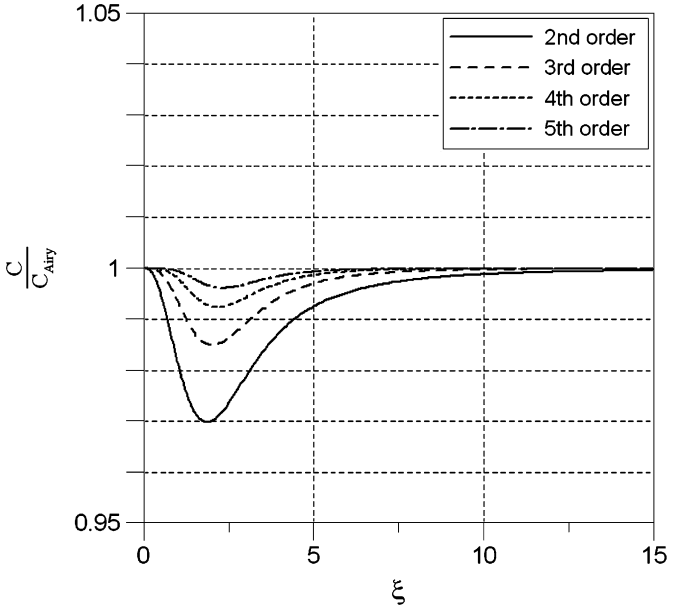

Fig. 2. Comparison of normalized phase velocities for different orders of $P(\xi)$ of Hunt formula.

where

$$\xi = \frac{\sigma^2 h}{g} \quad (30)$$

While denoting $P(\xi) = \sum_{j=0}^{S} d_j\xi^j$ with $d_0 = 1$ and defining the corresponding direct solution as Hunt's (1979) sth order approximate solution, the phase velocities for different Hunt's (1979) solution, normalized with respect to the phase velocity from the linear theory, are plotted as a function of ξ in Fig. 2 As shown in the figure, Hunt's solution approaches the solution of the linear dispersion equation as the order increases. However, the increase of the order makes the analytical solution much more complicated at the expense of a little improvement of accuracy. In addition, the convergence of the analytic solution can be judged analytically up to the fourth order, while a numerical method such as Bairstow's method (see Press et al., 1992, p. 370) should be used for the higher order solutions. Therefore, Hunt's fourth order solution is used in this study, the relative error of which is less than 1% for all values of ξ as shown in Fig. 2.

The coefficients of Eq. (27) are expressed with $P(\xi)$ and ξ as follows when Hunt's (1979) direct solution is used.

$$CC_g = \frac{g\tanh kh}{2k}\left(1 + \frac{2kh}{\sinh 2kh}\right) = \frac{g^2}{2\sigma^2}\frac{[P(\xi)+1]\xi}{\xi P(\xi)+1} \quad (31)$$

$$\frac{C_g}{C} = \frac{1}{2}\left(1 + \frac{2kh}{\sinh 2kh}\right) = \frac{P(\xi)+1}{2P(\xi)} \quad (32)$$

$$\frac{d(CC_g)}{dx} = \frac{dh}{dx}\frac{d}{dh}\left[\frac{g\tanh kh}{2k}\left(1 + \frac{2kh}{\sinh 2kh}\right)\right] + \frac{dh}{dx}\frac{dk}{dh}\frac{d}{dk}\left[\frac{g\tanh kh}{2k}\left(1 + \frac{2kh}{\sinh 2kh}\right)\right] = \frac{3g[P(\xi)+1] - 2g[\xi P(\xi)+1]}{2[P(\xi)+1][\xi P(\xi)+1]}\frac{dh}{dx} \quad (33)$$

Substituting Eqs. (31)–(33) and Eq. (5) into Eq. (27) yields the following approximate equation:

$$A(x)\frac{d^2\eta}{dx^2} + B(x)x^{\alpha_i-1}\frac{d\eta}{dx} + C(x)\eta = 0 \quad (34)$$

The variable coefficients $A(x)$, $B(x)$, and $C(x)$ are given in Appendix B. The solution of Eq. (34) can be obtained by duplicating the procedure from Eqs. (10) to (21).

The singular points, i.e., the roots for $A(x) = 0$, are as follows:

For $-b_1 < x \leqslant 0$

$$x^{\alpha_1} = (-1)^{\alpha_1}a_1^{\alpha_1} \quad (35)$$

$$x^{\alpha_1} = (-1)^{\alpha_1}\left(a_1^{\alpha_1} + \frac{1.63009 \pm 1.10252i}{\varepsilon_1}\right) \quad (36)$$

$$x^{\alpha_1} = (-1)^{\alpha_1}\left(a_1^{\alpha_1} - \frac{0.357769 \pm 1.98923i}{\varepsilon_1}\right) \quad (37)$$

$$x^{\alpha_1} = (-1)^{\alpha_1}\left(a_1^{\alpha_1} + \frac{1.9903 \pm 1.55755i}{\varepsilon_1}\right) \quad (38)$$

$$x^{\alpha_1} = (-1)^{\alpha_1}\left(a_1^{\alpha_1} - \frac{0.717978 \pm 2.10671i}{\varepsilon_1}\right) \quad (39)$$

For $0 < x \leqslant b_2$

$$x^{\alpha_2} = a_2^{\alpha_2} \quad (40)$$

$$x^{\alpha_2} = a_2^{\alpha_2} + \frac{1.63009 \pm 1.10252i}{\varepsilon_2} \quad (41)$$

$$x^{\alpha_2} = a_2^{\alpha_2} - \frac{0.357769 \pm 1.98923i}{\varepsilon_2} \tag{42}$$

$$x^{\alpha_2} = a_2^{\alpha_2} + \frac{1.9903 \pm 1.55755i}{\varepsilon_2} \tag{43}$$

$$x^{\alpha_2} = a_2^{\alpha_2} - \frac{0.717978 \pm 2.10671i}{\varepsilon_2} \tag{44}$$

where $\varepsilon_i = \sigma^2 h_0 / g a_i^{\alpha_i}$.

Since ε_i is positive because the lengths a_i are positive, the absolute values of x in Eqs. (35), (36), (38), (40), (41), and (43) are all greater than or equal to a_i. In Eqs. (37), (39), (42), and (44), x varies depending on ε_i, having the minimum value of $x = 0.94655a_i$ at $\varepsilon_i = 0.69$ in the case of $\alpha_i = 1$. Because the power series is used in the range of $0 \leqslant |x| \leqslant b_i$, the convergence of the series solution is guaranteed if $b_i < 0.94655a_i$. Since b_i is defined as $b_i = a_i \sqrt[\alpha_i]{1 - h_i/h_0}$, the series solution diverges only for very small values of h_i/h_0. Since this case is very rare, the present analytical solution converges in most practical situations.

In shallow water, the coefficients of Eq. (34) are reduced.

For $-b_1 < x \leqslant 0$

$$A(x) = 4(a_1^{\alpha_1} - (-1)^{\alpha_1} x^{\alpha_1}) \tag{45}$$

$$B(x) = -(-1)^{\alpha_1} 4\alpha_1 \tag{46}$$

$$C(x) = 4\nu_1^2 \tag{47}$$

For $0 < x \leqslant b_2$

$$A(x) = 4(a_2^{\alpha_2} - x^{\alpha_2}) \tag{48}$$

$$B(x) = -4\alpha_2 \tag{49}$$

$$C(x) = 4\nu_2^2 \tag{50}$$

With these coefficients, Eq. (34) becomes identical to Eq. (7) or Eq. (8).

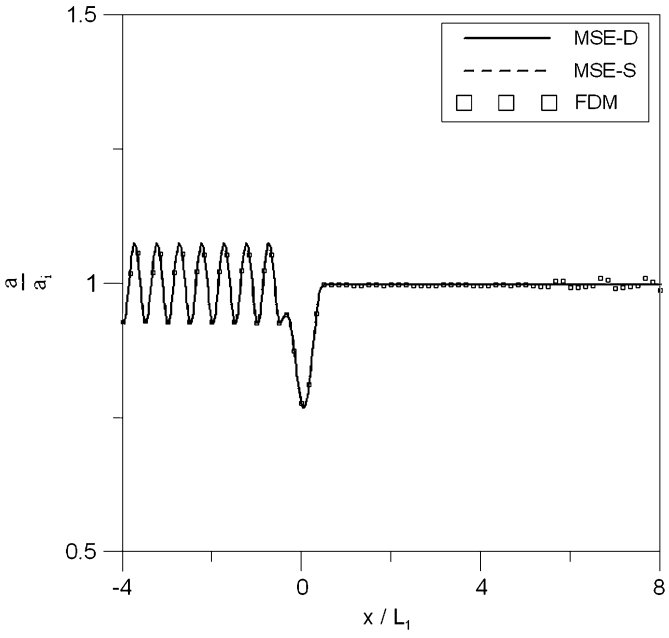

Fig. 3. Comparison among analytical and numerical solutions for normalized amplitudes for a symmetric trench with $\alpha_1 = \alpha_2 = 2$, $h_0 = 6.4$ m, $h_1 = h_2 = 3.2$ m, $b_1 = b_2 = 0.5L_1$, $k_1h_1 = 0.083$, and $k_0h_0 = 0.118$.

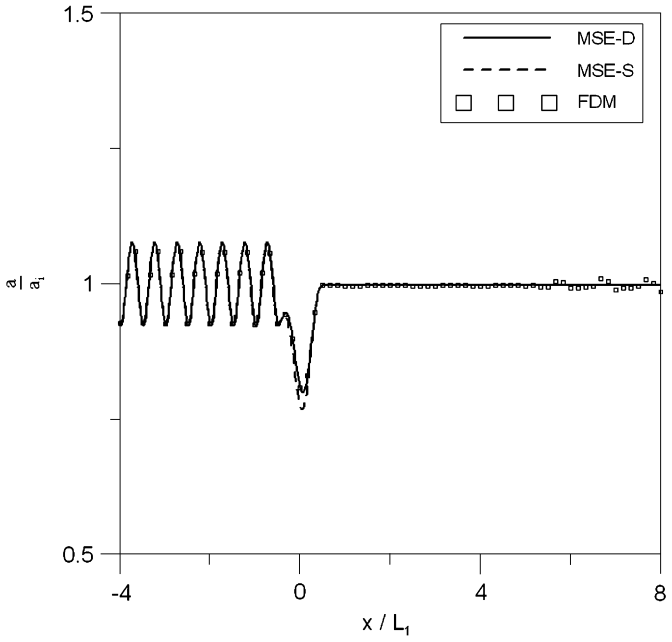

Fig. 4. Same as Fig. 3 except for $k_1h_1 = 0.334$ and $k_0h_0 = 0.481$.

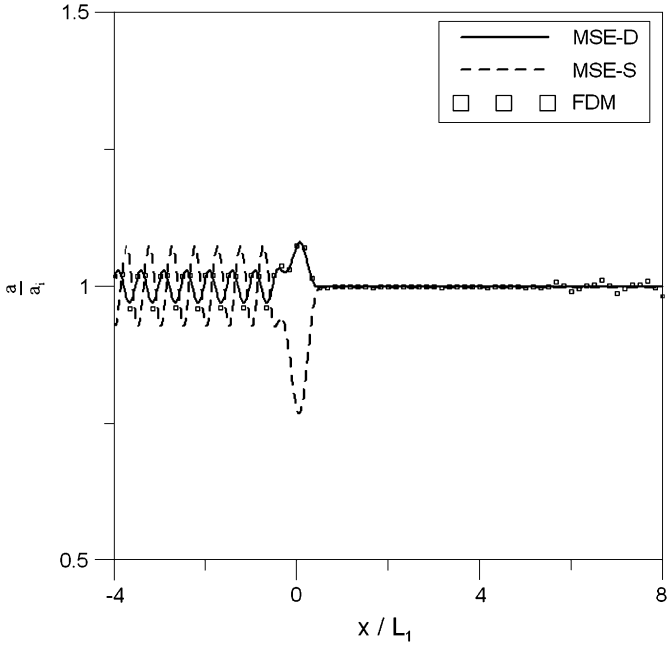

Fig. 5. Same as Fig. 3 except for $k_1h_1 = 1.336$ and $k_0h_0 = 2.368$.

3. Results and discussion

3.1. Comparison with numerical solutions

The long-wave solution and the mild-slope solution (hereafter MSE-S and MSE-D, respectively) are compared with the numerical solution based on the hyperbolic mild-slope equation developed by Copeland (1985). Computations are conducted for the following conditions: $\alpha_1 = \alpha_2 = 2$, $h_0 = 6.4$ m, $h_1 = h_2 = 3.2$ m, $b_1 = b_2 = 0.5\,L_1$, and k_1h_1 varies from 0.084 to 1.336 to consider a wide range of wave conditions. Figs. 3–5 show the comparisons of dimensionless wave amplitude among the MSE-S, MSE-D, and

the numerical model. When the longwave assumption is satisfied, three analytical solutions are almost identical to the numerical solution as shown in Fig. 3. However, as shown in Figs. 4 and 5, moving from shallow water to deeper waters, the mild-slope solution, MSE-D, still shows good agreement with the numerical solution, while the long-wave solution, MSE-S, shows large discrepancy with the numerical solution.

3.2. Miles's formula for wave reflection

The MSE-D was compared with the results from the Miles (1981) theory. Miles (1981) derived a theory for the wave reflection from an obstacle with small and continuous height variations by using the Fourier cosine transformation. The expression for reflection coefficients can be written as (Miles, 1981)

$$R_{\text{Miles}} = \left| \frac{2k^2}{2kh + \sin 2\,kh} \int_{-\infty}^{\infty} \delta(x) e^{2ikx} dx \right| \tag{51}$$

where $\delta(x)$ represents the bottom variation in the x-direction and can be expressed in this study as follows:

For $\alpha_i = 1$,

$$\delta(x) = \begin{cases} \frac{h_1 - h_0}{b_1} x & (0 \leqslant x < b_1) \\ \frac{(h_0 - h_2)(x - b_1) + (h_1 - h_0) b_2}{b_2} & (b_1 \leqslant x < b_1 + b_2) \end{cases} \tag{52}$$

For $\alpha_i \geqslant 2$,

$$\delta(x) = \begin{cases} h_0 \left(\frac{x^{\alpha_1} - 2b_1 x^{\alpha_1 - 1}}{a_1^{\alpha_1}} \right) & (0 \leqslant x < b_1) \\ \frac{h_1 a_2^{\alpha_2} - h_0 \{a_2^{\alpha_2} - (x - b_1)^{\alpha_2}\}}{a_2^{\alpha_2}} & (b_1 \leqslant x < b_1 + b_2) \end{cases} \tag{53}$$

The comparison was conducted for a simple case of $\alpha_1 = \alpha_2 = 2$, $b_1 = b_2 = 0.5L_{0.167}$, $h_1 = h_2 = 3.2$ m, and $h_0 = 3.2$ m, where $L_{0.167}$ represents the incident wave length when $k_1 h_1 = 0.167$ is satisfied. In the case of a symmetric trench, Eqs. (24) and (51) are expressed as follows:

$$R = \frac{-k_1^2 X_2(-b_1) X_1(b_1) - ik_1 X_2'(-b_1) X_1(b_1) + k_1^2 X_1(-b_1) X_2(b_1)}{\Delta} + \frac{ik_1 X_1'(-b_1) X_2(b_1) - ik_1 X_2(-b_1) X_1'(b_1) + X_2'(-b_1) X_1'(b_1)}{\Delta} + \frac{ik_1 X_1(-b_1) X_2'(b_1) - X_1'(-b_1) X_2'(b_1)}{\Delta} \tag{54}$$

$$R_{\text{Miles}} = \frac{2h_0}{a_1^2} \frac{k_1}{2k_1 h_1 + \sinh 2k_1 h_1} \times \left| \frac{b_1}{2ik_1} (e^{4ik_1 b_1} + 1) + \frac{1}{4ik_1^2} (e^{4ik_1 b_1} - 1) \right| \tag{55}$$

Fig. 6 shows the comparison of the reflection coefficients between the Miles (1981) theory and the present solution changing the incident wave period. Since the validity of the Miles (1981) theory is restricted to small variation of the bottom, the discrepancy between the two solutions increase as the central water depth in the trench increases. However, they show good agreement in relatively small height of the obstacle (i.e. $h_0 = 3.5$ m). As shown in Fig. 6, the magnitudes of the reflection coefficients increase and decrease periodically and their peak and span continuously decrease when the ratio of the half-width of a trench to the incident wave length increases. It is found that the peak and the span of reflection coefficients increase as the central water depth increases.

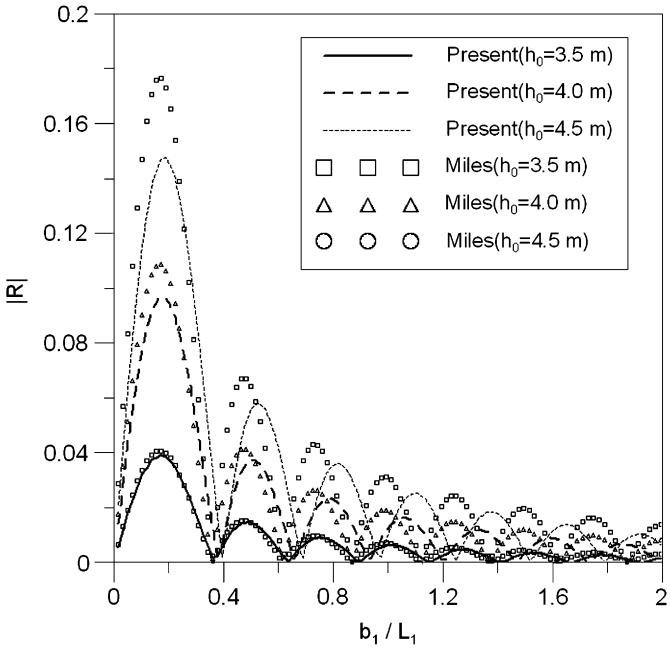

Fig. 6. Reflection coefficients of present and Miles solutions for different incident wave periods for the case of $\alpha_1 = \alpha_2 = 2$, $h_1 = h_2 = 3.2$ m, and $b_1 = b_2 = 0.5L_{0.167}$.

3.3. Effects of trench dimensions

In order to investigate the reflection of waves in detail, the reflection coefficients are calculated for various trench configurations. Fig. 7 shows the reflection coefficients calculated by changing the half-width of trench for different central water depths with the following geometrical and wave conditions: $\alpha_1 = \alpha_2 = 2$, $h_1 = h_2 = 3.2$ m, and $k_1 h_1 = 0.167$ and 1.336. Also, the central water depth varies from 6.4 to 12.8 m. In shallow water ($k_1 h_1 = 0.167$), the observed phenomena in Fig. 7 are similar to those of Fig. 6. The reflection coefficients increase and decrease periodically as the half-width increases, while the peak and span of reflection coefficients decrease. The peak and span of the reflection coefficient increase as the central water depth increases. In the intermediate-depth water ($k_1 h_1 = 1.336$), however, their span and peak are opposite to them in shallow water, which means that the peak increases while the span decreases as the central water depth increases.

Fig. 8 shows the reflection coefficients calculated by changing the central water depth for different half-widths of the trench in the same condition as in Fig. 7. The half-width of the trench varies from 0.25 to 1.0 L_1. In the shallow water, the results are somewhat contrast to Fig. 7. For instance, the peak and span of reflection coefficients increase as the central water depth increases and the peak of reflection coefficients decreases as the half-width of the trench increases. In the intermediate-depth water, the periodicity does not appear apparently within the computational range. And, the reflection seldom occurs when the half-width of the trench becomes equal to the incident wave length regardless of the central water depth.

The trench used in this study has the ability to deform to various shapes. For instance, when $\alpha_2 = 1$, $b_1 = 0$, $h_1 = 0.6$ m, and $h_2 = 0.2$ m, the trench becomes a constant-slope ramp used in Booij's (1983) test. When $b_1 = 0$ and $\alpha_2 \to \infty$ is satisfied, the trench becomes a step up and the reverse case is possible. And $\alpha_1 = \alpha_2 \to \infty$ gives a rectangular trench. In addition, analytical solutions for various shapes of trench can be obtained by adjusting the power

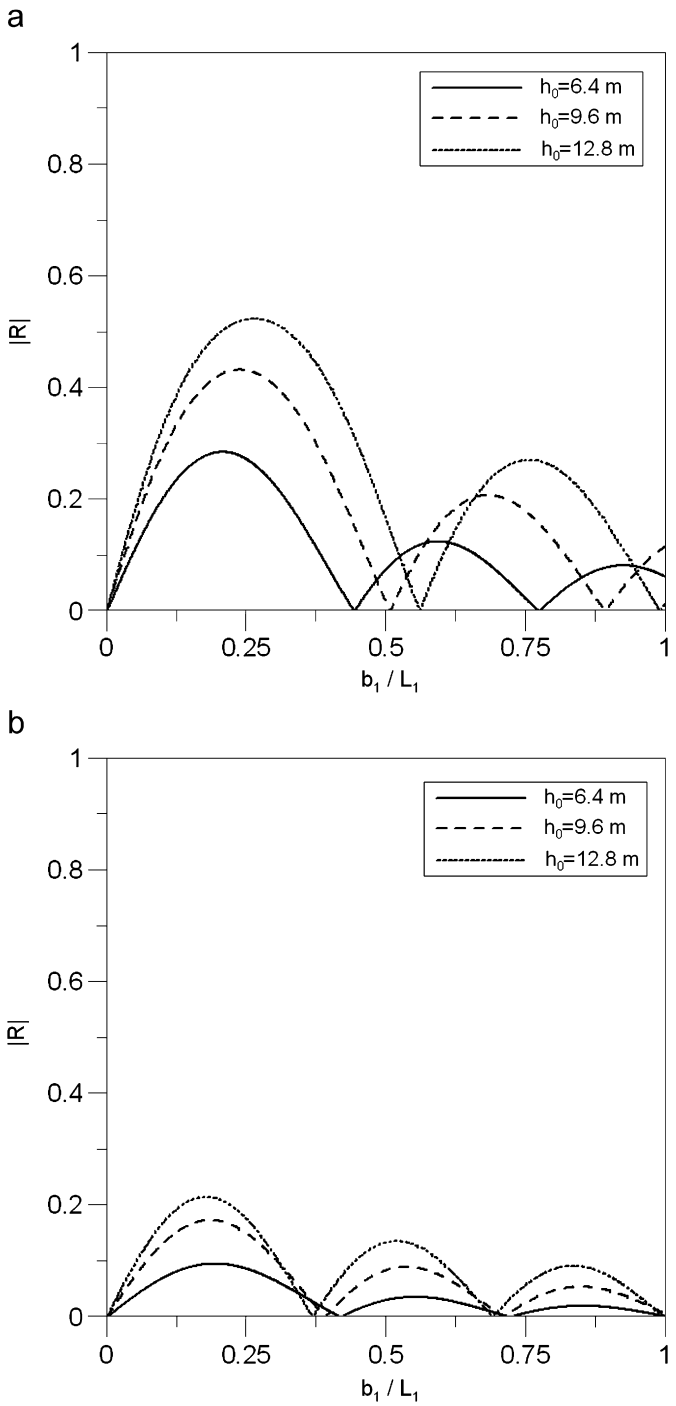

Fig. 7. Reflection coefficients of analytical solution for different central water depths for the case of $\alpha_1 = \alpha_2 = 2$, and $h_1 = h_2 = 3.2$ m: (a) $k_1 h_1 = 0.167$ and (b) $k_1 h_1 = 1.336$.

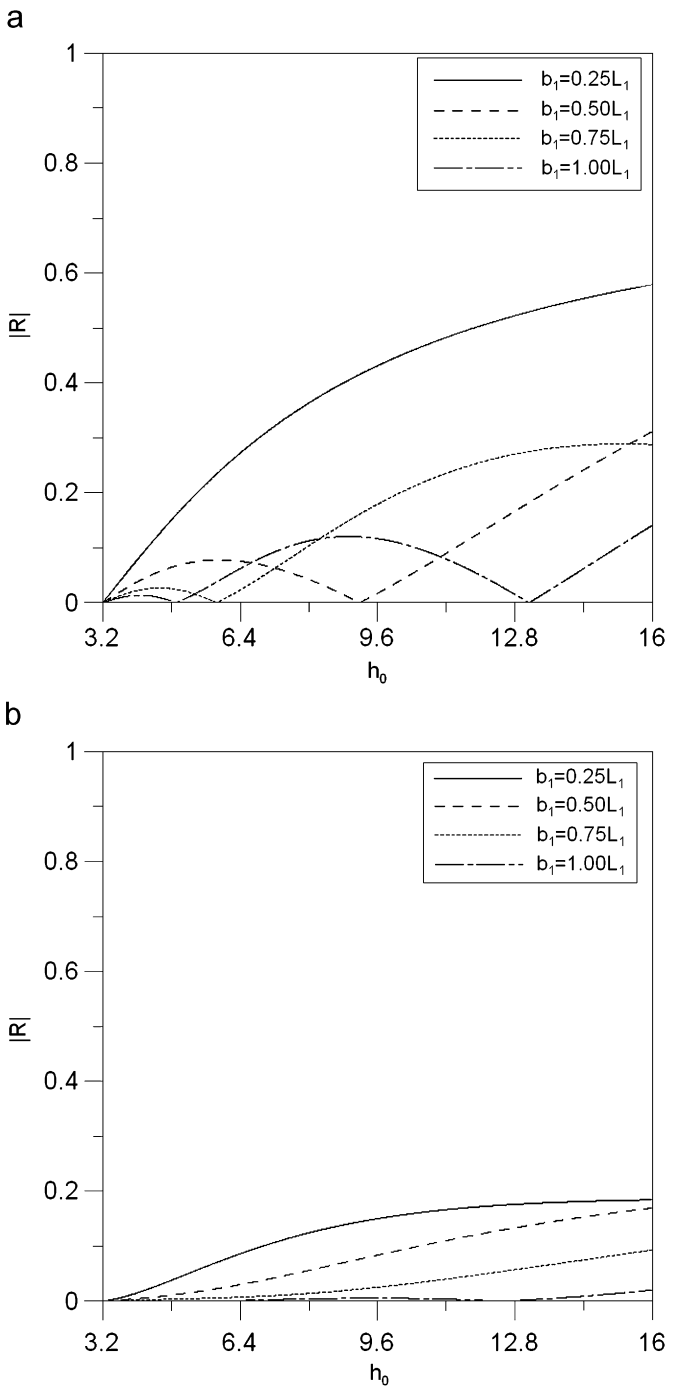

Fig. 8. Reflection coefficients of analytical solution for different half-widths of trench for the case of $\alpha_1 = \alpha_2 = 2$, and $h_1 = h_2 = 3.2$ m: (a) $k_1 h_1 = 0.167$ and (b) $k_1 h_1 = 1.336$.

of distance, the width of the trench, and the central water depth in both upwave and downwave sides.

4. Concluding remarks

Two types of analytical solutions have been derived in this study. One is the long-wave solution (MSE-S) and the other is a mild-slope solution (MSE-D). For the long-wave solution, the relationship $\sigma^2 = gk^2h$ based on the longwave assumption was used to make the coefficients of the governing equation explicit. In order to obtain a mild-slope solution, Hunt's (1979) explicit dispersion relation was used instead of the linear implicit dispersion relation. The convergence of the long-wave solution was guaranteed for all possible conditions. For instance, the analytical solution based on the longwave assumption gives the convergent solution for any given wave and geometric conditions, which satisfy the longwave assumption. The mild-slope solution converges in most cases except that the central water depth is much deeper in comparison to the constant water depth outside the trench. Therefore, it can be advocated that the present analytical solution is practical since the case in which the solution diverges is unusual.

The effects of the geometry of the trench on the reflection of waves were examined in both shallow and intermediate-depth waters. Similar phenomena to Bragg-reflection appeared. It is observed that the reflection coefficients increase and decrease periodically as one of the central water depth, the half-width of trench, or the incident wave period changes at the same time other parameters hold constant.

The analytical solutions developed in this study can be utilized for verifying the numerical solutions in addition to the analysis of the wave reflection and transmission. Since the numerical solutions inherently involve approximations, it is necessary to validate those models with the representative data. Analytical solutions are a direct examination of the numerical model scheme under idealized conditions. Also, they require relatively less cost, time, and efforts than the numerical or experimental methods.

Acknowledgements

This work was supported by the Korea Research Foundation Grant funded by the Korean Government (KRF-2006-311-D00887). The second writer was supported by the Project for Development of Reliability-Based Design Method for Port and Harbor Structures of Korea Ministry of Marine Affairs and Fisheries.

Appendix A. . Determination of $X_1(x)$ and $X_2(x)$

The coefficients of Eq. (16) can be expressed as

$$\beta_m = \frac{-(m-1)^2\beta_{m-1} - v_1^2\beta_{m-2}}{a_1 m(m-1)} = -\frac{(m-1)^2}{a_1 m(m-1)}\beta_{m-1} - \frac{v_1^2}{a_1 m(m-1)}\beta_{m-2} \quad (A.1)$$

Again, Eq. (A.1) can be expressed as follows:

$$\beta_0 = e_0\beta_1 + f_0\beta_0 \quad (A.2)$$

$$\beta_1 = e_1\beta_1 + f_1\beta_0 \quad (A.3)$$

$$\beta_m = c_m\beta_{m-1} + d_m\beta_{m-2} = e_m\beta_1 + f_m\beta_0 \quad (m \geqslant 2) \quad (A.4)$$

where

$$e_0 = 0, \quad f_0 = 1, \quad e_1 = 1, \quad f_1 = 0,$$
$$e_m = c_m e_{m-1} + d_m e_{m-2}, \quad f_m = c_m f_{m-1} + d_m f_{m-2},$$
$$c_m = -\frac{(m-1)^2}{a_1 m(m-1)}, \quad d_m = -\frac{v_1^2}{a_1 m(m-1)} \quad (A.5)$$

Therefore,

$$\begin{aligned}\eta_1 &= \sum_{m=0}^{\infty}\beta_m x^m = \beta_0 + \beta_1 x + \beta_2 x^2 + \beta_3 x^3 + \cdots \\ &= (e_0\beta_1 + f_0\beta_0) + (e_1\beta_1 + f_1\beta_0)x + (e_2\beta_1 + f_2\beta_0)x^2 \\ &\quad + (e_3\beta_1 + f_3\beta_0)x^3 + \cdots \\ &= (e_0 + e_1 x + e_2 x^2 + e_3 x^3 + \cdots)\beta_1 \\ &\quad + (f_0 + f_1 x + f_2 x^2 + f_3 x^3 + \cdots)\beta_0 \\ &= \beta_0 X_1(x) + \beta_1 X_2(x) \end{aligned} \quad (A.6)$$

where

$$X_1(x) = f_0 + f_1 x + f_2 x^2 + f_3 x^3 + \cdots \quad (A.7)$$

$$X_2(x) = e_0 + e_1 x + e_2 x^2 + e_3 x^3 + \cdots \quad (A.8)$$

Appendix B. . Variable coefficients

The expressions for $A(x)$, $B(x)$, and $C(x)$ in Eq. (34) are given as follows. In the following equations, $P(\xi)$ is given by Eq. (29) and is written here again for readability:

$$P(\xi) = 1 + \frac{2}{3}\xi + \frac{16}{45}\xi^2 + \frac{152}{945}\xi^3 + \frac{128}{2025}\xi^4 + \cdots \quad (29)$$

For $-b_1 < x \leqslant 0$

$$A(x) = [P(\xi)+1]^2 P(\xi)[a_1^{\alpha_1} - (-1)^{\alpha_1}x^{\alpha_1}] \quad (B.1)$$

$$B(x) = -(-1)^{\alpha_1}\alpha_1[3P(\xi) + 1 - 2P(\xi)\xi]P(\xi) \quad (B.2)$$

$$C(x) = \frac{\sigma a_1^{\alpha_1}}{g h_0}[P(\xi)\xi + 1][P(\xi)+1]^2 \quad (B.3)$$

where

$$\xi = \frac{\sigma^2 h}{g} = \frac{\sigma^2 h_0}{g a_1^{\alpha_1}}(a_1^{\alpha_1} - (-1)^{\alpha_1}x^{\alpha_1}) = \varepsilon_1(a_1^{\alpha_1} - (-1)^{\alpha_1}x^{\alpha_1}) \quad (B.4)$$

For $0 < x \leqslant b_2$

$$A(x) = [P(\xi)+1]^2 P(\xi)[a_2^{\alpha_2} - x^{\alpha_2}] \quad (B.5)$$

$$B(x) = -\alpha_2[3P(\xi) + 1 - 2P(\xi)\xi]P(\xi) \quad (B.6)$$

$$C(x) = \frac{\sigma a_2^{\alpha_2}}{g h_0}[P(\xi)\xi + 1][P(\xi)+1]^2 \quad (B.7)$$

where

$$\xi = \frac{\sigma^2 h}{g} = \frac{\sigma^2 h_0}{g a_2^{\alpha_2}}(a_2^{\alpha_2} - x^{\alpha_2}) = \varepsilon_2(a_2^{\alpha_2} - x^{\alpha_2}) \quad (B.8)$$

References

Bender, C.J., Dean, R.G., 2003. Wave transformation by two-dimensional bathymetric anomalies with sloped transitions. Coastal Engineering 50, 61–84.
Booij, N., 1983. A note on the accuracy of the mild-slope equation. Coastal Engineering 7, 191–203.
Bremmer, H., 1951. The W.K.B. approximation as the first term of a geometrical-optical series. Communications On Pure and Applied Mathematics 4, 105–115.
Chang, H.-K., Liou, J.-C., 2007. Long wave reflection from submerged trapezoidal breakwaters. Ocean Engineering 34, 185–191.
Cho, Y.-S., Lee, C., 2000. Resonant reflection of waves over sinusoidally varying topographies. Journal of Coastal Research 16, 870–879.
Copeland, G.J.M., 1985. A practical alternative to the mild-slope wave equation. Coastal Engineering 9, 125–149.
Dean, R.G., 1964. Long wave modification by linear transitions. Journal of the Waterways and Harbors Division 90 (1), 1–29.
Devillard, P., Dunlop, F., Souillard, B., 1988. Localization of gravity waves on a channel with random bottom. Journal of Fluid Mechanics 186, 521–538.
Hildebrand, F.B., 1976. Advanced Calculus for Applications, second Ed. Prentice-Hall, Englewood Cliff, NJ.
Hunt, J.N., 1979. Direct solution of wave dispersion equation. Journal of Waterway, Port, Coast. and Ocean Engineering 105, 457–459.
Kirby, J., Dalrymple, R.A., 1983. Propagation on oblique incident water waves over a trench. Journal of Fluid Mechanics 133, 47–63.
Kreisel, G., 1949. Surface Waves. Q. Appl. Math. 7, 21–44.
Lamb, H., 1932. Hydrodynamics, sixth Ed. Cambridge University Press.
Lassiter, J.B., 1972. The propagation of water waves over sediment pockets. Ph.D. thesis, Massachusetts Institute of Technology.
Lee, J.J., Ayer, R.M., 1981. Wave propagation over a rectangular trench. Journal of Fluid Mechanics 110, 335–347.
Lin, P., Liu, H.-W., 2005. Analytical study of linear long-wave reflection by a two-dimensional obstacle of general trapezoidal shape. Journal of Engineering Mechanics 131, 822–830.
Lin, P., Liu, H.-W., 2007. Scattering and trapping of wave energy by a submerged truncated paraboloidal shoal. Journal of Waterway, Port, Coast, and Ocean Engineering 133, 94–103.
Liu, P.L.-F., Cho, Y.-S., Kostense, J.K., Dingemans, M.W., 1992. Propagation and trapping of obliquely incident wave groups over a trench with currents. Appl. Ocean Res. 14, 201–212.

Liu, H.-W., Lin, P., Shankar, N.J., 2004. An analytical solution of the mild-slope equation for waves around a circular island on a paraboloidal shoal. Coastal Engineering 51, 421–437.

Mei, C.C., Black, J.L., 1969. Scattering of surface waves by rectangular obstacles in water of finite depth. Journal of Fluid Mechanics 38, 499–511.

Miles, J.W., 1967. Surface wave scattering matrix for a shelf. Journal of Fluid Mechanics 28, 755–767.

Miles, J.W., 1981. Oblique surface-wave diffraction by a cylindrical obstacle. Dynamics of Atmospheres and Oceans 6, 121–123.

Miles, J.W., 1982. On surface-wave diffraction by a trench. Journal of Fluid Mechanics 115, 315–325.

Press, W.H., Teukolsky, S.A., Vetterling, W.T., Flannery, B.P., 1992. Numerical Recipes in FORTRAN: The Art of Scientific Computing. Cambridge University Press.

Takano, K., 1960. Effects d'un obstacle parallelepipedique sur la propagation de la houle. Houille Blanche 15, 247.

Zhang, Y., Zhu, S., 1994. New solutions for the propagation of long water waves over variable depth. Journal of Fluid Mechanics 278, 391–406.